Journal of Mathematical Chemistry 15 (1994) 287–301

Application of the finite element method to time-dependent quantum mechanics: II. H_2^+ in a laser field

Hengtai Yu and André D. Bandrauk

Laboratoire de Chimie Théorique, Faculté des Sciences, Université de Sherbrooke, Sherbrooke, Québec, Canada J1K 2R1

Vijay Sonnad

Advanced Workstation Division, IBM Corporation, Austin, Texas, 78758, USA

Received 20 October 1993; revised 21 January 1994

A finite element method in Cartesian coordinates in three dimensions is described to solve the time-dependent Schrödinger equation for H_2^+ in the presence of time-dependent electromagnetic fields. The ionization rates, nonlinear optical polarizabilities and harmonic generation spectrum of H_2^+ have been calculated for field directions parallel or perpendicular to the hydrogen molecule ion axis. Comparisons of the present numerical results with previously published calculations show that the finite element method reproduces perturbative results and can treat nonperturbativity arbitrary intense short pulses as it includes automatically both bound and continuum electronic states.

1. Introduction

The interaction of intense external fields (intensity $\geqslant 10^{12}$ W/cm^2) with atoms and molecules leads to many interesting multiphoton phenomena such as above-threshold ionization and high-order harmonic generation. This has been an area of active research in the past decade [1–8]. The topic is a challenge for theoreticians since perturbation theories usually used are not valid for high intensity laser pulses [1,3]. Since the atomic unit of the electronic field e/a_0^2 corresponds to a field intensity of 3.5×10^{16} W/cm^2, current fields approaching 10^{14} W/cm^2 will introduce nonperturbative effects such as above threshold ionization [9] and laser-induced avoided crossings of molecular electronic potential curves [10,11]. In most experiments the electric-field amplitude can vary considerably on a scale of several cycles during the turn on of the pulse. Therefore, it is necessary to describe these high-intensity phenomena by solving numerically the time-dependent Schrödinger equation (TDSE). Previous theoretical papers published so far have used coordinates

in one or two dimensions or reduced the molecule-field system to the lower dimension by use of spherical, cylindrical or prolate-spheroidal coordinates in numerical solutions of TDSE [4–8,12–16].

One of the fundamental difficulties for describing nonperturbative time-dependent phenomena is the proper inclusion simultaneously of bound and continuum electronic states. In the case of the H atom, successful numerical calculations have been carried out by solving the TDSE using implicit finite difference (FD) methods in view of the local nature of the potential in the problem [4,8]. Extension of these numerical methods to multielectron problems has proved to be difficult due to the nonlocal nature of the exchange interaction.

Another approach which can handle nonlocal potentials is a basis set expansion, with sufficient flexibility to enable one to span localized bound state functions to highly delocalized free electron functions. Such flexible basis sets can be found in finite element (FE) methods which are local in nature. It is well known that simple FD and FE methods result often in identical approximations [17,18]. Recent applications of FE methods to time independent quantum chemistry has shown that these methods are well suited to treating nonlocal potentials such as the exchange potential in Hartree–Fock (HF) methods for atoms [19,20] and recently molecules [20–23]. In particular, taking advantage of expansion in terms of Legendre polynomials onto elements, one can obtain high accuracy due to the optimal properties of these polynomials: Legendre polynomials are the best approximation of any function with respect to its norm in a finite domain [24]. We have used such expansions in preliminary calculations of the time-dependent solution of the H and He atoms excited by an intense short laser pulse [12,13]. These calculations have been shown to compare extremely well with previous FD methods. The latter calculations are basis set free, whereas the FE method involves local basis sets. Current developments in time-independent basis-free quantum chemistry have shown these to be very promising [25,26], but have not yet been developped for time-dependent problems. In the present paper we describe the local basis FE method in Cartesian coordinates in 3 dimensions as applied to the solution of the TDSE for the hydrogen molecular ion in the presence of time-dependent electromagnetic perturbations. The Cartesian coordinates have the advantage of treating fields of arbitrary polarization. We are currently extending the method to the H_2 molecule and the H_3^+ molecular ion.

2. Theory

Clementi and collaborators [23] presented a FE method which they used for time-independent SCF calculations in Cartesian coordinates in three dimensions. We have rewritten this program using the KGNFLOW program from MOTECC90 [27] as a starting point for time-independent systems and extended it to time-dependent problems which allows one to efficiently manipulate large matrices.

2.1. TIME-INDEPENDENT EQUATIONS

The hydrogen molecular ion Schrödinger equation is of the form

$$H\Phi = E\Phi, \tag{1}$$

where Φ, the molecular orbitals of H_2^+, are expanded in a FE basis set,

$$\Phi = \sum_i C_i X_i . \tag{2}$$

$\{C_i\}$ and $\{X_i\}$ are the coefficient vector of the wave function and basis vector, respectively. The system Hamiltonian H is of the form

$$H = h_0 + \frac{1}{R_{ab}}, \tag{3}$$

R_{ab} is the distance between the two nuclei and h_0 is a single-electron Hamiltonian,

$$h_0 = -\frac{1}{2}\nabla^2 - \frac{1}{r_a} - \frac{1}{r_b}, \tag{4}$$

$$r_{a(b)} = \left[\left(z + (-)\frac{R_{ab}}{2}\right)^2 + x^2 + y^2\right]^{\frac{1}{2}}. \tag{5}$$

The variation of total energy E in eq. (1) with respect to the one-electron wave function leads to the SCF equations

$$\mathbf{FC} = E\mathbf{SC}, \tag{6}$$

where $\mathbf{C}$ is the coefficient vector, $\mathbf{F} = \mathbf{X}^+ h_0 \mathbf{X}$ is the Hamiltonian matrix and $\mathbf{S} = \mathbf{X}^+\mathbf{X}$ is the overlap matrix of the FE basis set.

Equation (6) is a generalized nonlinear eigenvalue equation. It can be solved by a SCF method. When Cartesian coordinates in three dimensions are used to solve the equation, the traditional finite element methods cannot be applied due to enormous storage and computing demands [23]. However we can use a block Lanczos method [28] to circumvent this problem. First, eq. (6) is transformed by left multiplication with $\mathbf{S}^{-1/2}$, and a new matrix equation is obtained,

$$\mathbf{AY} = E\mathbf{Y}, \tag{7}$$

where $\mathbf{A} = \mathbf{S}^{-1/2}\mathbf{F}\mathbf{S}^{-1/2}$ and

$$\mathbf{Y} = \mathbf{S}^{1/2}\mathbf{C}. \tag{8}$$

It is impossible to get the inverse of the overlap matrix $\mathbf{S}$ since the length of of the coefficient vector $\mathbf{C}$ in eq. (6) is usually greater than 10^4. We therefore introduce a high order approximation by use of Lobatto–Gauss basis sets, which are Lagrange interpolants on the set of k abscissas, of the k-point Lobatto–Gauss quadrature formula

$$b_j(k, w) = \prod_{i=1, i\neq j}^{k} \frac{(w - w_i)}{(w_j - w_i)} . \tag{9}$$

k is the polynomial order. Lobatto–Gauss basis sets have the orthonormal property

$$b_j(k, w_i) = \delta_{ij} . \tag{10}$$

Therefore the overlap matrix **S** can be approximated in this basis set by a vector which is only composed of diagonal terms of the overlap matrix **S**. Previous calculations show this approximation is very accurate in obtaining eigenvalues [23].

2.2. SINGULARITY IN NUCLEAR POTENTIAL

One difficulty in implementing FE methods for molecules, such as H_2^+, is the Coulomb potential at the location of the nuclei. If the nuclei are placed inside of the element, it is very difficult to remove the singularity. Therefore nuclei are always placed at the corner of the singular element. Clementi and collaborators [23] have presented a method in which a singular element is divided into three tetrahedra to remove the singularity. We have modified this method by using Duffy's method [29] as it leads to easier numerics.

The matrix elements of the nuclear potential we want to calculate in Cartesian coordinates in three dimensions are of the form

$$V_{ij} = \int_{-1}^{1}\int_{-1}^{1}\int_{-1}^{1} b_{i1}b_{i2}b_{i3}F(x, y, z)b_{j1}b_{j3}b_{j3}\,dx_1\,dx_2\,dx_3 , \tag{11}$$

where $b_{i(j)n}(n = 1, 2, 3)$ is the Lobatto–Gauss basis set, which are functions of the local coordinates x_n. Each $b_{i(j)n}$ is defined by eq. (9). The Coulomb potential $F(x, y, z)$ is a function of the global coordinates x, y, z and is of the form

$$F(x, y, z) = [x^2 + y^2 + z^2]^{-1/2} . \tag{12}$$

A relationship between local and global coordinates in the Cartesian coordinates in 3 dimensions is easily found,

$$x = c_1 + a_1x_1, \quad y = c_2 + a_2x_2, \quad z = c_3 + a_3x_3 , \tag{13}$$

where $c_i(i = 1, 2, 3)$ is the midpoint coordinate of the ith edge in the element considered, and $a_i(i = 1, 2, 3)$ is the half length of the ith edge. If the singular element is selected as a cube, then $a_1 = a_2 = a_3 = a$, therefore,

$$x = c_1 + ax_1, \quad y = c_2 + ax_2, \quad z = c_3 + ax_3 . \tag{14}$$

With the substitution

$$x_{11} = x_1 + 1, \quad x_{22} = x_2 + 1, \quad x_{33} = x_3 + 1 , \tag{15}$$

eq. (11) becomes

$$V_{ij} = \int_0^2 \mathrm{d}x_{11} \int_0^2 \mathrm{d}x_{22} \int_0^2 \mathrm{d}x_{33}\, b_{i1}b_{i2}b_{i3}F(x,y,z)b_{j1}b_{j32}b_{j3}\,. \tag{16}$$

This is an integral over a cube with an edge length of 2 and with a singularity at one of its corners. Now we divide this cube into 3 similar regions of which each region is a square bases pyramid, having one vertex at the origin and having one of the 3 opposite faces of the cube as a base. For the sake of simplicity, given that

$$f(x_{11},x_{22},x_{33}) = b_{i1}b_{i2}b_{i3}F(x,y,z)b_{j1}b_{j3}b_{j3}\,, \tag{17}$$

eq. (16) can be written as the sum of 3 integrals:

$$\begin{aligned} V_{ij} = &\int_0^2 \mathrm{d}x_{11} \int_0^{x_{11}} \mathrm{d}x_{22} \int_0^{x_{11}} \mathrm{d}x_{33} f(x_{11},x_{22},x_{33}) \\ &+ \int_0^2 \mathrm{d}x_{22} \int_0^{x_{22}} \mathrm{d}x_{33} \int_0^{x_{22}} \mathrm{d}x_{11} f(x_{11},x_{22},x_{33}) \\ &+ \int_0^2 \mathrm{d}x_{33} \int_0^{x_{33}} \mathrm{d}x_{11} \int_0^{x_{33}} \mathrm{d}x_{22} f(x_{11},x_{22},x_{33})\,. \end{aligned} \tag{18}$$

Relabelling the variables in the latter two integrals in above equation, we have

$$V_{ij} = \int_0^2 \mathrm{d}x_{11} \int_0^{x_{11}} \mathrm{d}x_{22} \int_0^{x_{11}} \mathrm{d}x_{33} \sum_{i=1}^{3} f_i\,, \tag{19}$$

where f_i's are cyclic permutations,

$$\sum_{i=1}^{3} f_i = f(x_{11},x_{22},x_{33}) + f(x_{22},x_{33},x_{11}) + f(x_{33},x_{22},x_{11})\,. \tag{20}$$

Changing variables,

$$x_{22} = \tfrac{1}{2}x_{11}u, \quad x_{33} = \tfrac{1}{2}x_{11}w\,, \tag{21}$$

eq. (19) becomes

$$V_{ij} = \tfrac{1}{4}\int_0^2 \mathrm{d}x_{11} \int_0^2 \mathrm{d}u \int_0^2 \mathrm{d}w\, x_{11}^2 (f_1 + f_2 + f_3)\,. \tag{22}$$

Changing the variables again,

$$r = x_{11} - 1, \quad s = u - 1, \quad t = w - 1\,, \tag{23}$$

we obtain

$$V_{ij} = \frac{1}{4}\int_{-1}^1 \mathrm{d}r \int_{-1}^1 \mathrm{d}s \int_{-1}^1 \mathrm{d}t\, (r+1)^2 (f_1 + f_2 + f_3) = \sum_i^3 P_i\,, \tag{24}$$

where

$$P_i = \frac{1}{4}\int_{-1}^{1} dr \int_{-1}^{1} ds \int_{-1}^{1} dt\,(r+1)^2 f_i\,. \tag{25}$$

When the nuclei are placed at the corner of an element, we can always perform a transformation such that $c_1 = c_2 = c_3 = a$. Therefore we obtain from the above equations

$$F = \frac{2}{a(r+1)}[4 + (s+1)^2 + (t+1)^2]^{-1/2}\,. \tag{26}$$

Putting eq. (26) into eq. (25), we obtain

$$P_i = \frac{1}{2a}\int_{-1}^{1} dr \int_{-1}^{1} ds \int_{-1}^{1} dt\,(r+1) b_{i1} b_{i2} b_{i3} b_{j1} b_{j3} b_{j3} [4 + (s+1)^2 + (t+1)^2]^{-1/2}\,, \tag{27}$$

where

$$b_{i(j)n} = b_{i(j)n}(r, \tfrac{1}{2}(r+1)(s+1) - 1, \tfrac{1}{2}(r+1)(t+1) - 1), \quad (n = 1, 2, 3)\,. \tag{28}$$

There is now no singularity in eq. (27) and P_i is easy to calculate. We thus can use the same matrix–vector multiple procedures as in the previous application [23], to avoid the storage of any matrix as we do in a nonsingular element. The nuclei may be placed at any corner of the singular element. The above method is valid as long as the nuclei are placed at the corner. When a midpoint coordinate $c_i (i = 1, 2, 3)$ values is less than 0, we need only to change the corresponding coordinate sign in $b_{i(j)n}$.

In table 1 we present some orbital energies and total energy of the ground state of H_2^+ using the present method, with 324 elements, $27 \times 27 \times 41$ degrees of freedom, and a box size $= \pm 6, \pm 6, \pm 8$ au in the directions of x, y, and z, respectively. The results in table 1, when compared with previous noncartesian FE calculations on H_2^+ [23,30] show excellent agreement. The analytical solution for H_2^+ is known: the ground state at equilibrium is $1\sigma_g$ and the total energy [30] is -0.6026 au. When the highest order of polynomial in each basis set is of 6 (in this paper), the total energy is -0.6023 au. When the order of polynomial is increased to 7 [31], the total energy is given by -0.6025 au, thus indicating convergence.

Table 1
Calculated energies for H_2^+ at $R = 1.9972$ au.

States	E (au)	Previous work (au) [a]	Exact value (au) [b]
$\sigma_g 1s$	−1.10297369	−1.10296601	
$\sigma_u^* 1s$	−0.66700430	−0.66689090	
$\pi_u 2p$	−0.42830026	−0.42348863	
Total ground state energy	−0.60227606	−0.60226503	−0.6026

[a] Ref. [23].
[a] Ref. [30].

2.3. TIME-DEPENDENT EQUATIONS

The time-dependent Schrödinger equation (TDSE) for H_2^+ is of the form [5]

$$i\frac{\partial}{\partial t}\Psi(r,t) = (h_0 + V^{ex})\Psi(r,t) = \mathbf{H}(r,t)\Psi(r,t)\,, \tag{29}$$

where h_0 is the Hamiltonian for the time-independent system, studied in the previous section and the $\Psi(r,t)$ are the time-dependent orbitals, which we express as

$$\Psi(r,t) = \mathbf{X}(r)\mathbf{C}(t)\,, \tag{30}$$

where $\mathbf{X}(r)$ is the time-independent FE basis set matrix and $\mathbf{C}(t)$ is the time-dependent coefficient vector. For linearly polarized laser fields and using Cartesian coordinates in three dimensions, the external electromagnetic perturbation V^{ex} will be written as

$$V^{ex} = E_0(t)z\sin(\omega t)\,, \tag{31}$$

if the external laser field is parallel to the hydrogen molecule ion axis (z), or as

$$V^{ex} = E_0(t)y\sin(\omega t)\,, \tag{32}$$

if the external laser field is perpendicular to that axis. $E_0(t)$ is called the pulse envelope for an electromagnetic field of frequency ω and both expressions (31) and (32) are written in the dipole approximation [3], i.e. the field has no spatial dependence.

Substituting eq. (30) into eq. (29), we readily obtain

$$i\frac{\partial}{\partial t}\Psi = i\mathbf{X}\dot{\mathbf{C}} = \mathbf{H}\Psi = \mathbf{H}\mathbf{X}\mathbf{C}\,. \tag{33}$$

Multiplying eq. (33) from the left by $\mathbf{X}^+$ and defining

$$\mathbf{B} = \mathbf{S}^{-1}\mathbf{X}^+\mathbf{H}\mathbf{X}\,, \tag{34}$$

we get finally the simple time-dependent matrix differential equation,

$$i\dot{\mathbf{C}} = \mathbf{B}\mathbf{C}\,, \tag{35}$$

where $\mathbf{S}^{-1}$ is the inverse of the overlap matrix (see eq. (6)).

The reduced equation (35) needs to be propagated from some initial time $t = 0$ to some final time t after we get the initial coefficient vector $\mathbf{C}(0)$ from eq. (6). Because the total Hamiltonian matrix has large dimensions, it is impractical to use a diagonalization procedure [5,32] to propagate eq. (35). As we did for H and He [12,13], the time-dependent coefficient vector $\mathbf{C}(t)$ is propagated successively by a fourth order Taylor series expansion from time $n\Delta t$ to $(n+1)\Delta t$,

$$\mathbf{C}^{n+1} = \left(1 - i\Delta t\mathbf{B} - \Delta t^2\mathbf{B}^2 + i\frac{1}{3!}\Delta t^3\mathbf{B}^3 + \frac{1}{4!}\Delta t^4\mathbf{B}^4\right)\mathbf{C}^n\,. \tag{36}$$

This involves multiplication of matrices only. The final wave function after a time

$t, \Psi(r, t, E(t))$ becomes an exact implicit function of the electromagnetic field $E(t)$ and is next used to calculate the exact field induced polarizability. In all calculations, an absorbing potential is used to avoid the reflections of the wave function propagated from the edges of the box. Such absorption removes ionizing electrons and allows for calculating ionization rates [5]. The propagation scheme (36) is always checked for convergence and normalization by choosing appropriate small time steps.

3. Results and discussion

In our previous work [12,13], we showed that the FE basis successfully gave highly accurate ionization rates and hyperpolarizabilities for the H and He atoms. In all our calculations for H_2^+, the center of the hydrogen molecular ion is placed in the center of a rectangular box. The sizes of the rectangular box are 24, 24, 60 and 30, 60, 24 au in x, y and z directions for fields $E(t)$ parallel (z) and perpendicular (y) to the axis of H_2^+, respectively. The box is divided into 144 elements and 8959 basis functions are used to propagate for the parallel field case, and 160 elements and 9639 basis functions for the perpendicular case. One laser field cycle is discretized in time with $n = 10^3$ points ($\tau = 2\pi/\omega, \Delta\tau = \tau/10^3$).

3.1. IONIZATION RATES

At the beginning of propagation ($t = 0$), the probabilities of occupancy of the 1s state is equal to 1 and the probabilities of all other states are equal to 0. Electrons are excited from the 1s state to other states of high energy while the wave functions are propagated. Therefore ionization rates can be calculated from the decrease of the probabilities of occupancy of the 1s state. These are calculated for long time using the formula $-\ln P(t) = \Gamma$, where $P(t)$ is the time dependent probability of the initial state.

The H_2^+ ionization rates Γ obtained for various intensities and field directions (z and y) are reported in table 2 together with other known results based on FD methods [5]. Both FD and FE results agree very well for the laser pulses parallel to the axis of the hydrogen molecular ion, i.e. the z-axis.

The variation of probabilities of the initial $1\sigma_g$ state with time are given in figs.

Table 2
Ionization rates Γ of H_2^+ at $R = 1.9972$ au for various intensities I (frequency $\omega = 0.0856$ au).

I (W/cm^2)	Γ_z (s^{-1}) this paper	Γ_z (s^{-1}) previous work [a]	Γ_y (s^{-1}) this paper
5×10^{14}	1.3×10^{12}	1.4×10^{12}	3.9×10^{11}
10^{15}	4.5×10^{13}	4.6×10^{13}	1.2×10^{13}

[a] Ref. [5], box size: $d = 64$ au.

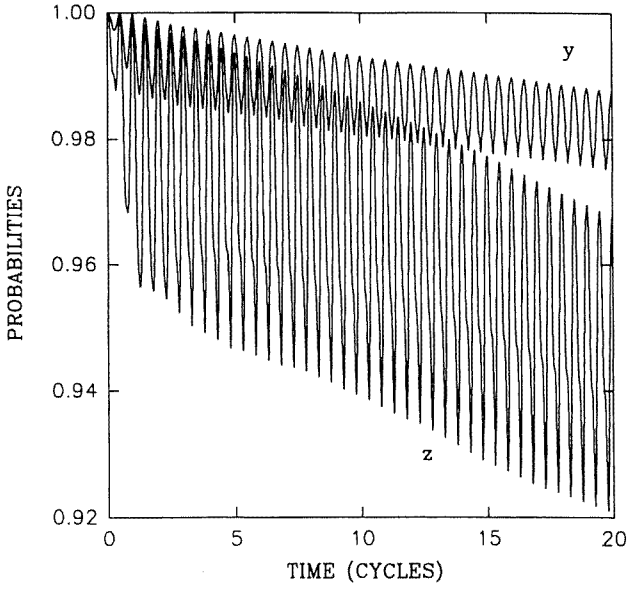

Fig. 1. Probabilities of ground state as a function of time for directions perpendicular (y) and parallel (z) to the H_2^+ axis: $I = 5 \times 10^{14}$ W/cm^2, frequency $\omega = 0.0856$ au. (1 optical cycle $= 1.8 \times 10^{-15}$ s.)

1 and 2 for the laser intensities 5.0×10^{14} and 1.0×10^{15} W/cm^2, respectively. It can be seen from these two figures that the slopes and amplitudes of oscillation of the probabilities of the $1\sigma_g$ state are clearly different at the same laser frequencies

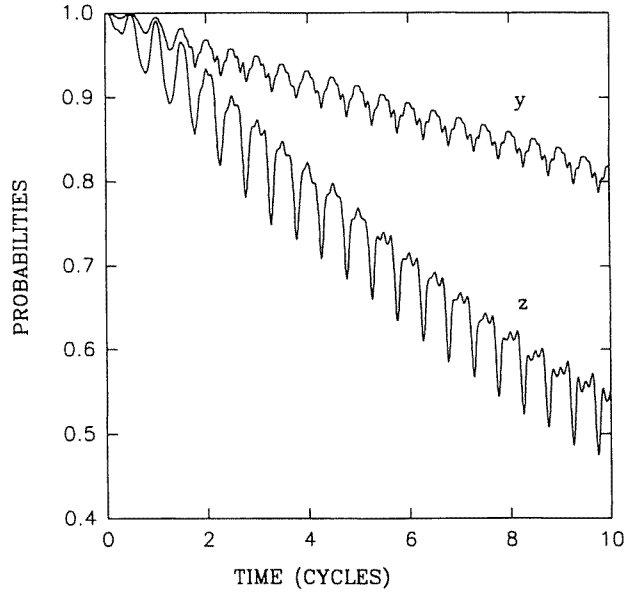

Fig. 2. same as Figure 1, $I = 10^{15}$ W/cm^2.

and intensities but for different directions: parallel (z) and perpendicular (y) to the molecular axis. When the laser field is parallel to the axis of H_2^+, the wave function expands with time along the molecular axis, z, whereas when the laser field is perpendicular, the wave function expands perpendicular to that axis. From both figs. 1 and 2, we infer that the interaction of the laser pulses with the hydrogen molecular ion are stronger in the direction parallel to the axis of H_2^+ than in the perpendicular direction due to the large extension of the wave function in the z-direction. This phenomena can be also seen from the electronic dipole moments, $d(t) = \langle \Psi(t) | d | \Psi(t) \rangle$, where $d = z$ or y are different directions shown in fig. 3. For the same laser intensity 5×10^{13} W/cm^2 and frequency 0.0856 au, the induced dipole moments parallel to z (H_2^+ axis) are larger than those perpendicular (y) to that axis. This correlates well with the different ionization rates (table 2) in the two directions. Both ionization rates and dipole moments perpendicular (y) to the internuclear axis (z) are reported here for the first time.

3.2. POLARIZABILITIES

When a molecule is exposed to the laser field, a complicated polarization takes place. The cloud of the electronic charge is deformed to accommodate the external field so that the molecule, even though symmetric, acquires an induced dipole moment and polarizabilities. However, the calculations of polarizabilities are much more difficult than those of ionization rates since the former demands not only more calculations as a function of field amplitude but also more precision.

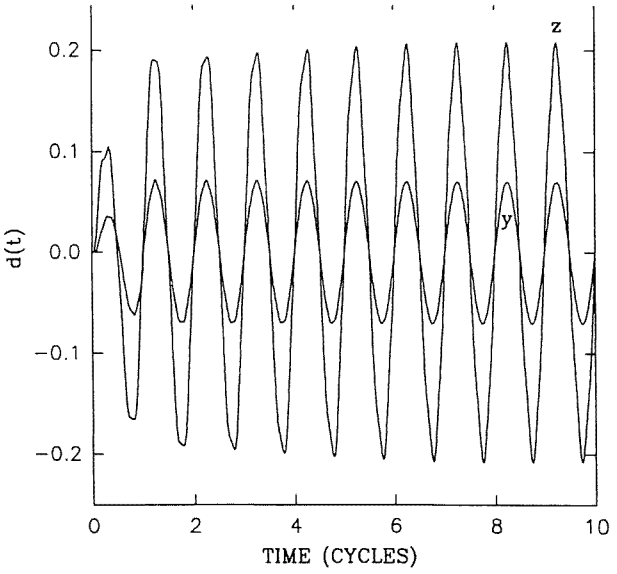

Fig. 3. Comparison of the perpendicular (y) to the parallel (z) dipole moment at the intensity $I = 5 \times 10^{13}$ W/cm^2 and frequency $\omega = 0.0856$ au.

Most previous calculations of polarizabilities of atoms and small molecules, generally rely on time-independent iterations or perturbations, for example H [33,34], He [35,36], noble gases [37–39], alkali metals [40] and small molecules [41–43]. Here we present the first result of calculations based on numerical solutions of the TDSE, using FE basis sets in Cartesian coordinates in 3 dimensions.

The electronic polarizabilities of the hydrogen molecular ion have been calculated previously [42–48], but the results contradict each other. For example, Bishop and collaborators [46,47] have calculated the value of $\gamma_{\|} = 41$ au and Adamowicz and collaborators [43] obtained a value of $\gamma_{\|} = 2300$ au. We follow our previous method [13] for H and He to calculate these in Cartesian coordinates in 3 dimensions.

In general, the electronic polarizability or dipole moment induced in an atom or molecule by a uniform external field $E(t)$ can be expressed in a power series expansion [49],

$$d(t) = \langle \Psi(t)|d|\Psi(t)\rangle = \alpha E(t) + \frac{\gamma}{3!}E(t)^3 + \ldots . \tag{37}$$

The range of the intensity of the laser pulses used to calculate the polarizabilities varies from 10^{13} to 10^{14} W/cm^2 for both the frequencies $\omega = 0.0856$ and $\omega = 0.0428$ au and for the two directions: z and y. In the parallel case (z direction), 8 intensities are used and 1500 points per cycle for each intensity are collected. In the perpendicular case (y), 6 intensities and the same number of points are used. The results calculated have been checked for convergence. The present results and previous published results are given in table 3. It can be seen from table 3 that our results are very close to those calculated by Bishop and collaborators [46], in both parallel and perpendicular directions. We note that most previous published results are static results, i.e. $\omega = 0$. All our results are dynamic ($\omega \neq 0$).

Table 3
Hyperpolarizabilities of the hydrogen molecular ion (units: au) at $R = 1.9972$ au.

ω	$\alpha_{\|}$	$\alpha_{\perp}$	$\gamma_{\|}$	$\gamma_{\perp}$
0.0428	5.13	1.82	−44.4	80.0
0.0856	5.29	1.84	−70.0	106.0
Previous results				
0.01	5.84 [a]		−193 [a]	
0.0	5.84 [b]		2300 [b]	83.8 [c]
0.0	5.078 [d]	1.758 [d]	−40.9 [e]	73.04 [e]
0.0	5.199 [f]	1.829 [f]		

[a] Ref. [42], averaged over the vibrational ground state.
[b] Ref. [43].
[c] Ref. [44].
[d] Ref. [45].
[e] Ref. [46,47].
[f] Ref. [48].

3.3. HARMONIC GENERATION

In a very intense laser pulse, an atom or molecule can radiate at multiples or harmonics of the incident laser frequency. This process which is usually called optical harmonic generation has been observed experimentally and calculated by FD methods for atoms only [4]. We present for the first time the harmonic generation spectrum of H_2^+ for both field polarizations, z and y. These are nonperturbative results which can only be obtained by the present method.

Harmonic generation spectra are given for the laser intensity 5×10^{14} W/cm^2 and frequency 0.0856 au in figs. 4 and 5 for parallel (z) and perpendicular (y) directions, respectively. These spectra are defined from the power spectrum

$$|d(\omega)|^2 = \left| \int_{-\infty}^{\infty} e^{i\omega t} d(t)\, dt \right|^2 . \tag{38}$$

The intensity of the laser light increases from 0 to a maximum during the first optical cycle, and is then kept constant. The results shown in figs. 4 and 5 are obtained for a time of 5–20 optical cycles. Each figure reveals a series of peaks at odd multiples of the laser frequency, extending to at least the 45th harmonic. If we compare the harmonic spectra in fig. 4 with those in fig. 5, it can be seen that the intensities of the harmonic spectra with the laser field parallel to the axis (z) of H_2^+ are stronger than those with the laser field perpendicular (y) to that axis, by about one order of magnitude. This is in agreement with the calculations of the dipole moments, fig. 4. In fact, experiments measuring angular distributions of protons

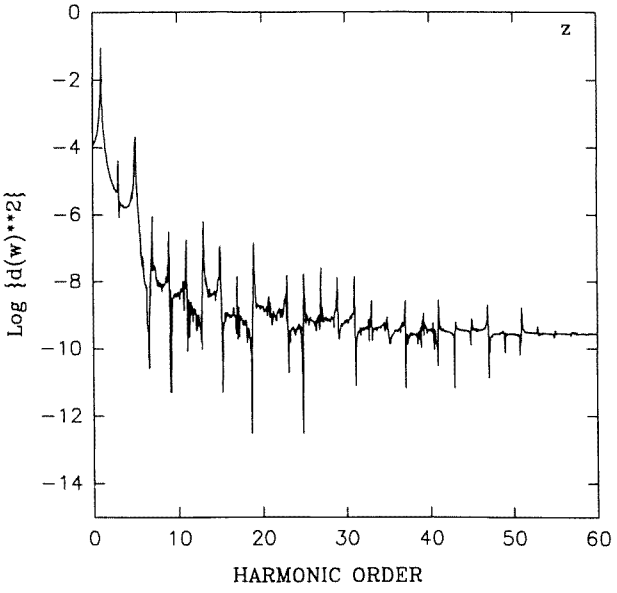

Fig. 4. Harmonic spectra of the hydrogen molecular ion with the laser field parallel (z) to molecule axis at the intensity $I = 5 \times 10^{14}$ W/cm^2 and frequency $\omega = 0.0856$ au.

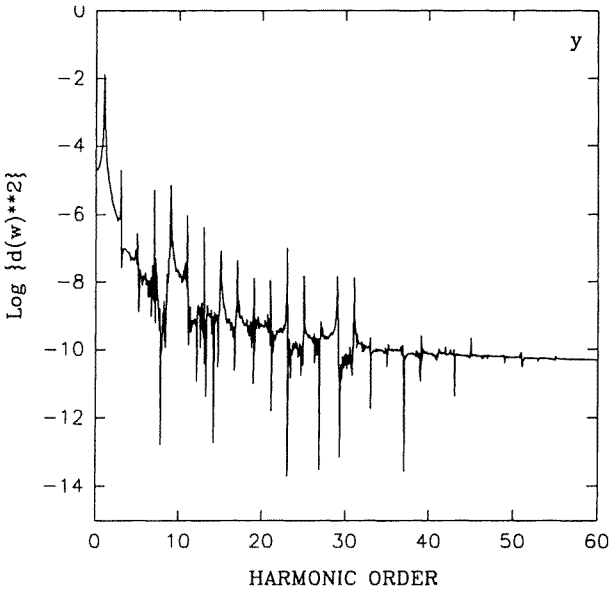

Fig. 5. Harmonic spectra of the hydrogen molecular ion with the laser field perpendicular (y) to the molecule axis at the intensity $I = 5 \times 10^{14}$ W/cm^2 and frequency $\omega = 0.0856$ au.

emitted during the multiphoton ionization of the H_2 molecule show that the protons are always tightly focused along the polarization axis of the laser field [9]. This means that the molecule absorbs photons most efficiently when it is aligned with the external field. This is a result of large charge transfer transitions such as $1\sigma_g \rightarrow 1\sigma_u$ for which the transition moment diverges as $R/2$ [3,10,11]. Our calculated results are in agreement with this fact. It is interesting to note that harmonic spectra in the perpendicular (y) direction in fig. 5 show us also an initial sharp drop-off intensity, followed by a rather broad plateau, and then a sudden cut-off. These features are characteristic of atomic optical harmonic spectra, both theoretical [4,15] and experimental [50,51]. We further note that $\gamma_\perp > \gamma_\parallel$ is in agreement with figs. 4 and 5 where the third harmonic is weaker for parallel polarization than the other harmonics.

4. Conclusions

The ionization rates, nonlinear optical polarizabilities and harmonic generation spectra of H_2^+ in Cartesian coordinates in 3 dimensions have been calculated non-perturbatively using FE methods for field directions parallel and perpendicular to the hydrogen molecule ion axis. We present for the first time nonperturbative ionization rates for excitations perpendicular to the molecular axis. The results obtained here, including those previously calculated for H and He atoms [12,13] show that FE basis sets which are local in nature are ideally suited to treat nonper-

turbative time-dependent problems for time-dependent perturbations which lead to high excitations into Rydberg and continuum states. Our numerical calculations of low order hyperpolarizabilities agree well with previous perturbative calculations and offer the possibility of calculating high order ones since our basis sets, which allow for calculation of ionization rates, therefore implicitly contain continuum state contributions. We are currently extending the FE method to the time-dependent quantum mechanics of the H_2 and the H_3^+ ion.

Our calculations so far do not include the motion of the nuclei. Rotation is very slow on the time scale of ionization so it can be neglected. But vibrations of the nuclei in the molecule should be taken into account, from which vibrational contributions to low order hyperpolarizabilities are expected [46]. This aspect is being currently pursued in a nonperturbative approach.

Acknowledgements

We thank Prof. J.K. Cullum [28] for providing her Lanczos program. The financial support from the Centre of Excellence in Molecular and Interfacial Dynamics and the Natural Sciences and Engineering Research Council of Canada is gratefully acknowledged.

References

[1] A.D. Bandrauk (ed.), *Atomic and Molecular Processes with Short Intense Laser Pulses*, NATO ASI, Vol. B171 (Plenum Press, New York, 1988).
[2] A.D. Bandrauk and S.C. Wallace (eds.), *Coherence Phenomena in Atoms and Molecules in Laser Fields*, NATO ASI, Vol. B278 (Plenum Press, New York, 1992).
[3] A.D. Bandrauk, *Molecules in Laser Fields* (Marcel Dekker, New York, 1993).
[4] J.L. Krause, K.J. Schafer and K.C. Kulander, Chem. Phys. Lett. 178 (1991) 573.
[5] S. Chelkowski, T. Zuo and A.D. Bandrauk, Phys. Rev. A46 (1992) 5342.
[6] M.S. Pinzola, C.J. Bottrell and C. Bottcher, J. Opt. Soc. Am. B7 (1990) 659.
[7] P.L. Devries, J. Opt. Soc. Am. B7 (1990) 519.
[8] K.C. Kulander, Phys. Rev. A36 (1987) 2726.
[9] P.H. Buchsbaum, A. Zavriyev, H.G. Muller and D.W. Schumacher, Phys. Rev. Lett. 64 (1990) 1883.
[10] A.D. Bandrauk and M.L. Sink, Chem. Phys. Lett. 57 (1978) 569; J. Chem. Phys. 74 (1981) 1110.
[11] E. Aubanel, A.D. Bandrauk and P. Rancourt, Chem. Phys. Lett. 197 (1992) 419.
[12] H. Yu, A.D. Bandrauk and V. Sonnad, in ref. [2], p. 31.
[13] H. Yu, A.D. Bandrauk and V. Sonnad, Part I of this paper, J. Math. Chem. 15 (1994) 273.
[14] M. Horbatsch, Phys. Rev. A44 (1991) 5346.
[15] J.H. Eberly, Q. Su and J. Javanainen, Phys. Rev. Lett. 62 (1989) 881.
[16] K. LaGattuta, Phys. Rev. A41 (1991) 5157.
[17] B.A. Finlayson, *Method of Weighted Residues* (Academic Press, New York, 1974).
[18] O.C. Zinkiewicz and K. Morgan, *Finite Elements and Approximation* (Wiley, New York, 1983).

[19] D. Sundholm, J. Olsen and S.A. Alexander, J. Chem. Phys. 96 (1992) 5229.
[20] D. Heinemann, A. Rosen and B. Fricke, Chem. Phys. Lett. 166 (1990) 627.
[21] D. Heinemann, B. Fricke and D. Kolb, J. Chem. Phys. 38 (1988) 4994.
[22] T. Inoshita, Phys. Rev. B41 (1990) 180.
[23] H. Murakami, V. Sonnad and E. Clementi, Int. J. Quant. Chem. 42 (1992) 785.
[24] G. Hammerlin and K.H. Hoffmann, *Numerical Methods* (Springer, New York, 1991).
[25] A.D. Becke, J. Chem. Phys. 76 (1982) 6037.
[26] A.D. Becke and R.M. Dickson, J. Chem. Phys. 92 (1990) 3610.
[27] E. Clementi (ed.), *Modern Technique in Computational Chemistry: MOTECC90* (1990) chap. 12.
[28] J.K. Cullum and R.A. Willoughby, *Lanczos Algorithms for Large Symmetric Eigenvalue Computations*, Vol. II, Program (Birkhauser, New York, 1985).
[29] M.G. Duffy, SIAM. J. Numer. Anal. 19 (1982) 1260.
[30] I.L. Levine, *Quantum Chemistry*, 3rd Ed. (Allyn and Bacon, Newton, Massachusetts, 1983).
[31] H. Yu, A.D. Bandrauk and V. Sonnad, to appear in Chem. Phys. Lett. (1994).
[32] A.D. Bandrauk and H. Shen, J. Chem. Phys. 99 (1993) 1185.
[33] N.C. Manakov, M.A. Preobrazhenskii and L.P. Rapoport, Opt. Spectr. 35 (1973) 14.
[34] C.A. Nicolaides, T. Mercouris and G. Aspromallis, J. Opt. Soc. Am. B7 (1990) 494.
[35] Y. Justum, A. Maquet and Y. Heno, Phys. Rev. A41 (1990) 2791.
[36] L.L. Boyle, A.D. Buckingham, R.L. Disch and D.A. Dunmur, J. Chem. Phys. 45 (1966) 1318.
[37] P. Sitz and R. Yaris, J. Chem. Phys. 48 (1968) 3546.
[38] P.R. Taylor, T.J. Lee, J.E. Rice and J. Almlof, Chem. Phys. Lett. 163 (1989) 359.
[39] M. Jaszunski and D.L. Yeager, Phys. Rev. A40 (1989) 1651.
[40] J.E. Rice, P.R. Taylor, T.J. Lee and J. Almlof, J. Chem. Phys. 94 (1991) 4972.
[41] R.B. Miller and S.E. Harris, IEEE J. Quant. Electr. QE-9 (1973) 470.
[42] D.M. Bishop, J. Pipin and J.N. Silverman, Mol. Phys. 59 (1986) 165.
[43] L. Adamowicz and R.J. Bartlett, J. Chem. Phys. 84 (1986) 4988.
[44] D.M. Bishop and B. Lam, Chem. Phys. Lett. 134 (1987) 283.
[45] D.M. Bishop and L.M. Cheung, J. Phys. B11 (1978) 3133.
[46] D.M. Bishop, Rev. Mod. Phys. 62 (1990) 343.
[47] D.M. Bishop and L.M. Cheung, J. Phys. B12 (1979) 3135.
[48] P.R. McEachran, S. Smith and M. Cohen, Can. J. Chem. 52 (1974) 3463.
[49] Y.R. Shen, *The Principles of Nonlinear Optics* (Wiley, New York, 1984).
[50] M. Ferry, A. L'Huillier, X. Li, L.A. Lompré, G. Mainfray and C. Manus, J. Phys. B21 (1988) L31.
[51] X.F. Li, A. L'Huillier, M. Ferry, L.A. Lompré, G. Mainfray, Phys. Rev. A39 (1989) 3751.